Available online at www.sciencedirect.com
SCIENCE DIRECT®
Biochimica et Biophysica Acta 1613 (2003) 49–56
BIOCHIMICA ET BIOPHYSICA ACTA
BBA
www.bba-direct.com

Residues 45 and 404 in the murine reduced folate carrier may interact to alter carrier binding and mobility

Rongbao Zhao, Yanhua Wang, Feng Gao, I. David Goldman*

Departments of Medicine and Molecular Pharmacology, Albert Einstein College of Medicine Cancer Center, Chanin 2, 1300 Morris Park Ave., Bronx, NY 10461, USA

Received 3 October 2002; received in revised form 14 April 2003; accepted 30 April 2003

Abstract

The reduced folate carrier (RFC), a facilitative transporter, plays a major role in the delivery of reduced folates and antifolates into cells. Previous studies indicated that mutations of E45K in the first transmembrane domain (TMD), and K404L in the 11th TMD, produce selective and opposite alterations in binding of natural folate substrates to murine RFC. The former mutation is frequently associated with antifolate resistance. The current study was designed to determine whether there might be an interaction between these sites by comparing the transport properties of RFC-null cell lines stably transfected with K404E, E45K, or E45K/K404E carriers. These studies demonstrated that: (1) All mutant carriers were inserted into the plasma membrane. (2) In the K404E mutant, the influx K_t's for 5-formyltetrahydrofolate and 5-methyltetrahydrofolate were markedly increased, and to a much smaller extent folic acid, as compared to L1210 cells. However, with introduction of a second E45K mutation the influx K_t for these folates reverted to those of the E45K cells which retained wild-type binding for 5-methyltetrahydrofolate and enhanced binding of 5-formyltetrahydrofolate and folic acid. (3) The influx V_{max} of the E45K mutant was markedly reduced. Introduction of the second K404E mutation doubled this parameter and the ratio of V_{max} to K_t for 5-formytetrahydrofolate was restored to ~ 50% that of the wild-type carrier consistent with a substantial increase in function. (4) Chloride inhibits wild-type RFC but the E45K mutant requires chloride for activity. The K404E mutant is also suppressed by chloride but introduction of the K404E mutation decreased the chloride-dependence of E45K. The results suggest that there is an interaction between the E45 and K404 residues in the first and 11th TMDs, respectively, but that the E45 residue appears to be the more dominant determinant of binding and anion sensitivity.

Keywords: Residue; Folate; Carrier

1. Introduction

The reduced folate carrier (RFC-SLC19A1) is a member of the Major Facilitator Superfamily [1] and the major transporter for 5-CH_3-THF, the folate present in the plasma of man and rodents [2]. RFC is essential for mouse development and its deletion by homologous recombination results in early embryonic lethality [3]. RFC is also the major route for the delivery of antifolates into tumor cells and an important determinant of the efficacy of these agents [4]. RFC generates uphill transport of folates through an exchange mechanism that appears to be linked to organic anions concentrated within cells [5,6]. From a structural perspective, murine RFC is predicted to have 12 transmembrane domains (TMDs), with its N and C termini oriented to the cytoplasm; a similar topology had been proposed for the human carrier [7,8]. However, recently, an alternative topology for TMD 9–12 of human RFC was presented based upon hemagglutinin epitope and scanning glycosylation insertion mutagenesis [9].

There has been considerable interest in identifying RFC residues that are important determinants of function and binding specificity. The first TMD has emerged as an important site; in particular residues 45, 46, and 48 in mRFC [10–12]. An E45K substitution in the murine and human carriers with antifolate selective pressure, noted by several groups, resulted in markedly decreased carrier mobility, a change in the spectrum of substrate specifities (decreased affinity for methotrexate (MTX), increased affinity for folic acid and 5-CHO-THF), and an obligatory

Abbreviations: 5-CH_3-THF, 5-methyltetrahydrofolate; 5-CHO-THF, 5-formyltetrahydrofolate; HBS, HEPES buffered saline; MTX, methotrexate; RFC, the reduced folate carrier; TMD, transmembrane domain

* Corresponding author. Tel.: +1-718-430-2302; fax: +1-718-430-8550.
E-mail address: igoldman@aecom.yu.edu (I.D. Goldman).

0005-2736/03/$ - see front matter © 2003 Elsevier Science B.V. All rights reserved.
doi:10.1016/S0005-2736(03)00136-6

requirement for inorganic anions unlike the wild-type carrier that is markedly inhibited by a variety of inorganic and organic anions [10,13,14]. Systematic substitution of glutamate-45 of murine RFC with other amino acids further characterized the properties of this residue that are important to carrier function [15].

Other charged residues in RFC TMDs also play an important role in carrier function. Substitution of arginine-131, -155, or -336 with leucine, by site-directed mutagenesis, abolished RFC activity. However, replacement of K404 with leucine in the 11th TMD maintained affinity for MTX but markedly reduced affinity for 5-CHO-THF and 5-CH_3-THF and decreased the inhibitory effects of chloride on RFC function [16]. Replacement of lysine-411 in human RFC (corresponding to lysine-404 in murine RFC) with arginine, glutamate, or leucine also decreased RFC function although E411R was as active as the wild-type carrier in transporting 5-CHO-THF [17].

Because glutamate-45 and lysine-404 are oppositely charged and appear to play important but largely opposite roles in determining the specificity of folate binding and anion sensitivity, studies were undertaken to assess whether there might be an interaction between these residues that determines the configuration of the folate binding site, its anion sensitivity, and/or whether one of these sites might play a dominant role in these processes. This paper evaluates these possibilities by describing the properties of mutant carriers in which residues were substituted either with the oppositely charged species, E45K, K404E, or both mutations—E45K/K404E. The results suggest that there is an interaction between these residues in the first and 11th TMDs but the E45 residue appears to be the dominant determinant of binding and anion sensitivity.

2. Materials and methods

2.1. Chemicals

[3′, 5′, 7-^{3}H]-(6*S*)-5-CHO-THF was obtained from Moravek Biochemicals (Brea, CA), and [3′, 5′, 7-^{3}H]-MTX was purchased from Amersham Corp. (Arlington Heights, IL). Unlabeled MTX and 5-CHO-THF were provided by Lederle (Carolina, Puerto Rico) while folic acid and 5-CH_3-THF were purchased from Sigma (St. Louise, MO). Both tritiated and unlabeled compounds were purified by high performance liquid chromatography before use [18]. All other reagents were of the highest purity available from various commercial sources.

2.2. Cell culture conditions and cell lines

A variety of L1210 murine leukemia cell lines were utilized in these studies. These include: (i) the MTX^{r}A subline with an A130P mutation that markedly impaired RFC function [19]; (ii) the D10 subline without RFC protein because of a mutation in the ATG start codon [20,21]; (iii) the R16 subline, an RFC-transfectant derived from MTX^{r}A that has high-level carrier expression [22]. The E45 cells were previously reported [10], K404E and E45K/K404 mutant lines are described below. All cells were grown in RPMI-1640 medium containing 2.3 μM folic acid, supplemented with 5% bovine calf serum (HyClone), 2 mM glutamine, 20 μM 2-mercaptoethanol, penicillin (100 units/ml), and streptomycin (100 μg/ml) at 37 °C in a humidified atmosphere of 5% CO_2. Transfectants were cultured in the same medium supplemented with 750 μg/ml of G418.

2.3. Site-directed mutagenesis of RFC

Site-directed mutagenesis was carried out according to the QuickChange protocol from Strategene as reported previously [15]. For constructing K404E and E45K/K404E expression vectors, RFC-pCDNA 3.1 and RFC-E45K-pCDNA 3.1 were used as templates, respectively [10]. A pair of complementary oligonucleotides (5′-CTACTGCGCTTGAGACCTGTAACTC-3′ and 5′-GTGATACAGGTCTCAAGCGCAGTAG-3′), which contains an altered codon for position-404 (K404E), was used as the primers in this protocol. The targeting vectors obtained (RFC-K404E-pcDNA3.1 and RFC-E45K/K404E-pcDNA3.1) were sequenced in the Albert Einstein Cancer Center DNA Sequencing Facility. They harbor only the targeted mutations. Large amounts of plasmid DNA used for transfections were prepared using Wizard Plus Midipreps (Promega).

2.4. Transfections

MTX^{r}A (1×10^7 cells) were electroporated (300 V, 200 μF) with 50 μg of nonlinearized pcDNA3.1 (+) containing the mutated RFC cDNA in a final volume of 800 μl of serum-free RPMI-1640 medium. Cells were then diluted in 20 ml of complete RPMI-1640 medium, allowed to recover for 48 h, adjusted to 2×10^5 cells/ml in medium containing G418 (750 μg/ml active drug), and then distributed into 96-well plates at approximately 4×10^4 cells/well. Seventeen and nine G418-resistant clones were obtained for K404E and E45K/K404E construct transfections, respectively. One K404E transfectant and one E45K/K404E transfectant were selected for further studies because these two cell lines demonstrated the highest level of MTX influx activity in each group. The transfectants were maintained in RPMI-1640 medium containing 750 μg/ml G418.

2.5. Northern blot analysis

Total RNA was isolated from the transfectants, MTX^{r}A, and L1210 cells using the TRIzol reagent (Invitrogen). RNA (20 μg) was resolved by electrophoresis on 1% agarose gels containing formaldehyde. The RNA was transferred to

Hybond-N nylon membrane (Amersham Life Science), cross-linked to the membrane by a Stratalinker (Stratagene), and hybridized first with murine RFC cDNA and then, after stripping, with actin cDNA. The radioactive blots were exposed to X-ray films overnight. Transcripts of both RFC and actin were also quantitated by PhosphorImager analysis to determine RFC message levels in the transfectants relative to L1210 cells.

2.6. Western blot analysis

A polyclonal antibody, AE390, to the distal C terminus of murine RFC (Met^{499} through Ala^{512}) was used to probe cell plasma membranes as reported [21]. Plasma membranes were isolated by sucrose gradient ultracentrifugation using a protease inhibitor cocktail (P8340, Sigma) at a dilution of 1:1000 instead of 1 mM phenylmethylsulfonylfluoride [23]. Protein concentrations of the total lysate and plasma membranes were determined with the BCA Protein Assay Kit (Pierce). The proteins were dissolved in a SDS-PAGE loading buffer (60 mM Tris, 10% glycerol (v/v), 2% SDS and trace bromophenol, pH 6.8) without heating and resolved on a 12% SDS-polyacrylamide gel. The proteins were transferred to PVDF Transfer Membranes and processed by the ECL Plus Western Blotting Detection System, both obtained from Amersham Life Science.

2.7. Immunofluorescence

Cells were harvested, washed with PBS buffer, and then fixed in 4% paraformaldehyde in PBS for 30 min at room temperature. Cells were then washed twice with PBS buffer and the cell pellets embedded in optimal cutting temperature compound (OCT) for frozen sections. For staining, sections were washed twice with PBS and incubated in 10% normal goat serum for 30 min at room temperature. After removing excess serum, the affinity purified AE390 antibody directed to the murine RFC C terminus [21] was added to the sections at a 1:50 dilution followed by incubation for 60 min at 4 °C. The sections were then washed in PBS at 4 °C overnight before incubation with fluorescein isothiocyanate (FITC)-conjugated anti-rabbit-IgG (Invitrogen) at a 1:500 dilution for 45 min at 4 °C. The sections were then washed five times with PBS buffer and mounted with ProLong Antifade solution (Molecular Probes). Photographs were obtained under fluorescence microscopy with a 40-fold magnification.

2.8. Transport assay

Influx measurements were performed by methods described previously [10] with minor modifications, in HEPES buffered saline (HBS) (20 mM HEPES, 140 mM NaCl, 5 mM KCl, 2 mM $MgCl_2$, 5 mM glucose, pH 7.4), HEPES-sucrose-MgO buffer (20 mM HEPES, 235 mM sucrose, pH 7.4 with MgO), or mixtures of both. Briefly, cells were harvested, washed twice with, and resuspended in, the appropriate buffer to a density of 1.5×10^7 cells/ml. Cell suspensions were incubated at 37 °C for 25 min, following which uptake was initiated by the addition of radiolabeled folate and samples taken at the indicated times. Uptake was terminated by injection of 1 ml of the cell suspension into 10 ml of ice-cold HBS. Cells were collected by centrifugation, washed twice with ice-cold HBS, and processed for measurement of intracellular radioactivity [22]. For influx determinations, uptake intervals were adjusted so that cell MTX did not exceed the DHFR binding capacity assuring that unidirectional uptake conditions were sustained. 5-CHO-THF initial rates were established over an interval in which cell folate uptake was linear as a function of time with an extrapolated ordinate intercept at time zero near the point of origin. 5-CHO-THF influx K_t and V_{max} were obtained from nonlinear regression of influx versus concentration according to the Michealis–Menten equation. Influx K_i's for MTX, 5-CH_3-THF, and folic acid were determined by Dixon-plot analysis based upon inhibition of 5-CHO-THF influx by these folate substrates in E45K, E45K/K404E, and L1210 cells. These parameters were assessed in K404E cells based upon inhibition of MTX influx by these folate substrates. The higher influx of MTX as compared to 5-CHO-THF in this cell line allowed more accurate transport measurements for this RFC substrate.

3. Results

3.1. Transfection and expression of the E45K, K404E, and E45K/K404E mutant RFC carriers in the folate transport-deficient MTX^rA line

cDNAs of mutated carriers E45K, K404E, and E45K/K404E were cloned into the mammalian expression vector pcDNA 3.1 and transfected into MTX^rA cells that lack endogenous RFC function [19]. Several clones were obtained for each transfection. The K404E and E45K/K404E transfected clones that demonstrated the highest MTX influx activities were chosen for further study and named K404E and E45K/K404E cells, respectively. Properties of the E45K transfectant (E45K cells) were previously reported [10].

Fig. 1A is a representative Northern blot of total RNA from K404E and E45K/K404E cells along with wild-type L1210 and recipient MTX^rA cells. The message derived from the expression vector in the transfectants was smaller than, but could not be separated from, endogenous transcript in MTX^rA and L1210 cells. To determine the relative RFC mRNA levels, Northern blots were quantitated by PhosphoImager analysis, normalized to actin levels, and then to the mRFC level in L1210 cells that was assigned a value of 1. mRNA contributed by endogenous RFC in recipient MTX^rA cells was subtracted from the levels in transfectants. RFC mRNA in the K404E and E45K/K404E cells was comparable to the level in L1210 cells with the former only

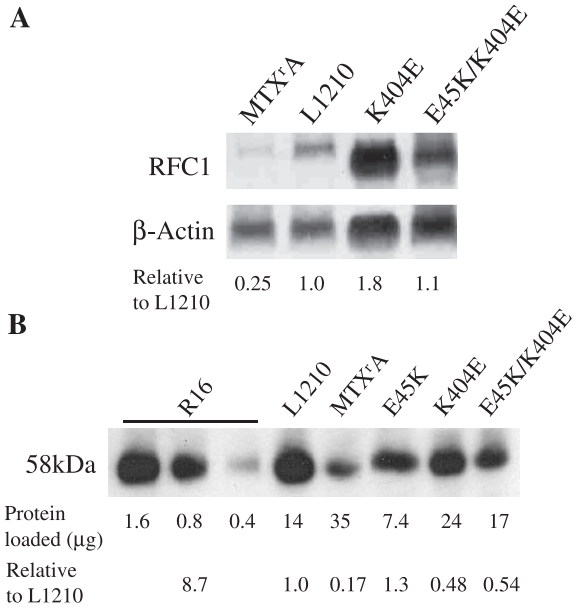

Fig. 1. (A) Northern blot analysis of total RFC RNA and (B) Western blot analysis of RFC protein in plasma membranes. (A) Total RNA was hybridized successively with the full-length RFC and β-actin cDNA. The data shown is a representative X-ray film. The level of transcripts was also quantitated by PhosphorImager analysis of radioactive blots and normalized to the levels of β-actin mRNA. The values indicated are the average of two such analyses with a difference of less than 10% for K404E and E45K/K404E cells. (B) Plasma membrane fractions isolated from transfectants were probed with antibody directed to the C-terminus of the RFC. The amount of plasma membrane loaded on the SDS-gel is indicated. Signals on the X-ray film were determined by Kodak Image Station 440. Signal changes in R16 cells as a function of RFC protein loaded were used to quantitate RFC expression levels in the other cells. The RFC expression levels relative to L1210 cells are indicated. The data are the average of two separate experiments with a difference of less than 30%.

slightly higher. RFC mRNA was 4.5 times greater in E45K cells than that in L1210 cells [10].

RFC protein in plasma membranes was assessed by Western blot analysis (Fig. 1B). To account for discrepancies in protein loading, different amounts of plasma membranes from R16 cells, in which RFC is overexpressed, were loaded in the same gel to serve as standards. In addition, amounts of plasma membranes from different cell lines loaded on the SDS-gel were adjusted in an attempt to minimize differences in the RFC signals. Consistent with the activity previously reported, R16 cells express ~ 9-fold greater RFC protein than L1210 cells [22]. RFC protein in MTX^{r}A was 1/6 the level of L1210 cells. RFC proteins in K404E and E45K/K404E were both about 1/2 the level of L1210 cells; E45K was 30% greater than L1210 cells. Hence, the ratio of RFC protein to RFC mRNA in all the transfectants is less than in L1210 cells.

Expression of RFC was also monitored in transfectants by immunofluorescence. As indicated in Fig. 2, no fluorescence was detected in D10 cells which completely lack RFC protein [20,21]. These cells served as a negative control. In MTX^{r}A cells, the recipient of the transfections, there was weak fluorescence that was not present in the plasma membrane. RFC was detected in wild-type L1210 cells mainly in the plasma membrane and, to a lesser extent, in the cytosol, but was predominant at the plasma membrane of R16 cells that overexpress wild-type RFC protein. Fluoresence in the E45K, K404E, and E45K/K404E cells was largely present at the plasma membrane although there was some cytosolic fluorescence as well; strong staining was found in only a portion of transfectants. Hence, like wild-type and R16 cells, the mutated carriers appeared

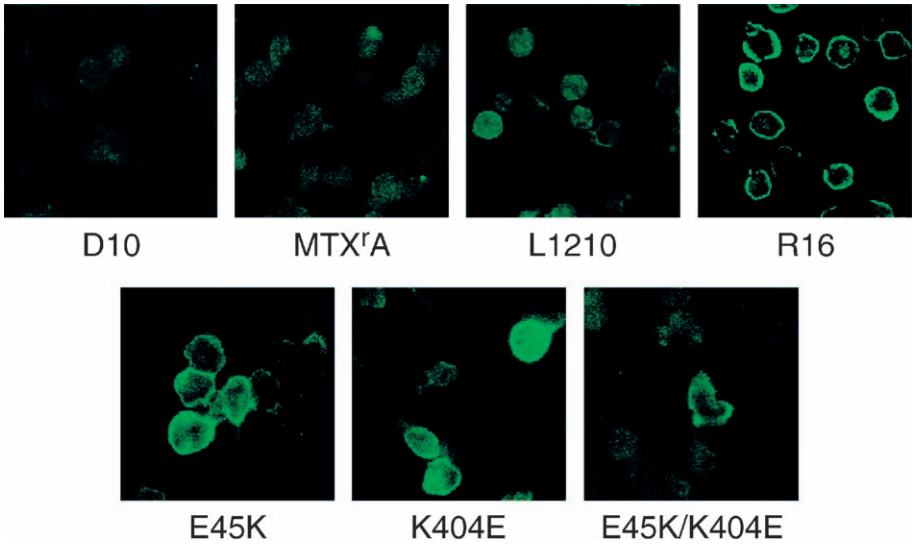

Fig. 2. Detection of RFC proteins by fluorescence microscopy. Cells were harvested, fixed and embedded in frozen sections. The sections were first incubated with an antibody directed to the C terminus of murine RFC and then with FTIC-conjugated anti-rabbit-IgG as described in Materials and Methods. The images represent a 40-fold magnification.

largely localized to the plasma membrane; there was no evidence for a trafficking defect.

3.2. Influx of MTX and 5-CHO-THF

MTX and 5-CHO-THF initial uptake rates normalized to the level of RFC protein in the plasma membrane were determined (Fig. 3A). In all transfectants, influx of MTX and 5-CHO-THF was lower than in L1210 cells, but greater than in MTX^{r}A cells, indicating that all mutants retained some function. As indicated in Fig. 3B, 5-CHO-THF influx was decreased by a factor of 5 in E45K cells and by a factor of 10 in K404E cells as compared to L1210 cells. However, influx in the double mutant was greater than in either mutant alone, twice the sum of the single mutants, and only 40% less than that of L1210 cells. The pattern for MTX influx was somewhat different. Influx in the E45K was 1/10 that of L1210 cells, but transport in the K404E was twice as fast (1/5 that of L1210 cells), a pattern that was the reverse of what was observed for 5-CHO-THF. Restoration of MTX transport in the double mutant was less than that for 5-CHO-THF. Hence, function was substantially restored for both folates when carrier harbored both mutations although the magnitude of restoration was greater for 5-CHO-THF.

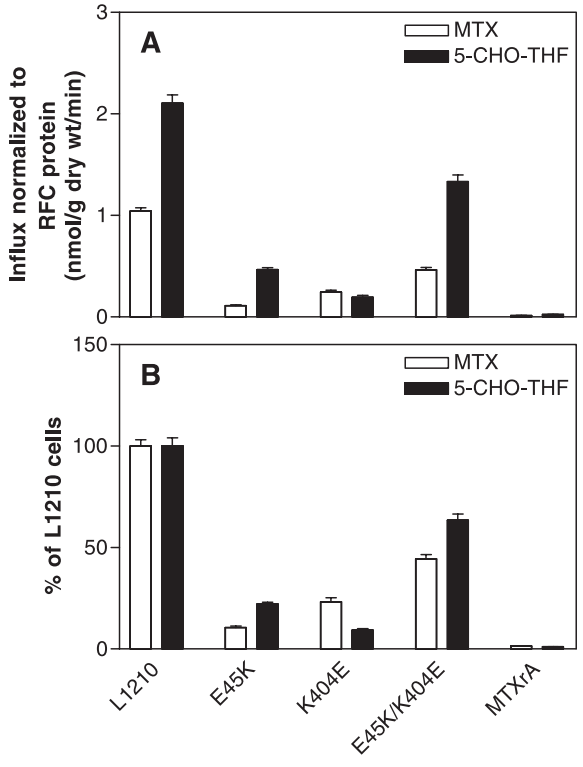

Fig. 3. Comparison of influx of [^{3}H]-MTX and [^{3}H]-5-CHO-THF. After 25-min incubation in HBS buffer at 37 °C, uptake was initiated by addition to the cell suspension of 1 μM [^{3}H]-MTX or [^{3}H]-5-CHO-THF and terminated by injecting 1 ml of the cell suspension into 9 ml of ice cold HBS. Influx is the slope of uptake as a function of time measured within 2 min for MTX and 1 min for 5-CHO-THF. (A) Initial uptake is normalized to the relative RFC expression levels indicated in Fig. 1B except for MTX^{r}A cells. (B) Initial uptake is further normalized to the percentage of wild-type L1210 cells indicated as 100%. Data are the average ± S.E. from three separate experiments.

Table 1
Comparison of 5-CHO-THF influx kinetic parameters in transfectants and L1210 cells

	K_t	V_{max}	V^*_{max}	V^*_{max}/K_t
L1210	5.4 ± 0.3	17.0 ± 1.6	17	3.2
E45K	1.5 ± 0.1	1.4 ± 0.1	1.1	0.73
E45K/K404E	1.5 ± 0.2	1.2 ± 0.1	2.2	1.5
K404E	55 ± 5 (K_i)	5.2 (calculated)	11	0.20

5-CHO-THF influx at substrate concentrations of 0.5, 1, 2, 3 or 5 μM was determined in E45K/K404E cells. Influx K_t (μM) and V_{max} (nmol/g dry wt/min) for E45K/K404E cells were obtained from nonlinear regression to the Michealis–Menten equation. These parameters for L1210 and E45K cells reported previously [10] were used for purpose of comparison. 5-CHO-THF influx K_i in K404E cells was determined from a Dixon plot analysis based upon inhibition of [^{3}H]-MTX influx by nonlabeled 5-CHO-THF. The 5-CHO-THF influx V_{max} in K404E cells was calculated from the Michealis–Menten equation based upon 5-CHO-THF influx at 1 μM and the assumption that the 5-CHO-THF influx K_t is equal to influx K_i. V^*_{max} indicates the values normalized to the relative RFC protein expression levels shown in Fig. 1B. Data are the mean ± S.E. from three separate experiments.

3.3. Influx kinetics

Folate influx kinetics was determined to quantitate the impact of the mutations on carrier affinities for the different folates and the mobilities of the RFC-folate complexes. As indicated in Table 1, the 5-CHO-THF influx K_t was decreased by a factor of ~3.6 in the E45K as reported previously [10] and the influx K_i was increased by a factor of 10 in the K404E mutant compared to the fourfold increase in K404L [16]. However, the K_t reverted to that of the E45K in the double mutant. The 5-CHO-THF influx V_{max} was normalized to the level of RFC in the plasma membranes of these cell lines. There was a marked reduction (15-fold) in the V_{max} for the E45K mutant. The V_{max} for the double mutant was twice that of the E45K but still far less than that of wild-type L1210 cells. Finally, while V_{max}/K_t was decreased by factors of 4.4 and 16 in the E45K and K404E cells, respectively, this value was restored to ~50% of L1210 cells in the E45K/K404E cells consistent with substantial preservation of function.

The influx K_i was also measured for MTX, 5-CH_3-THF, and folic acid based upon a Dixon analysis of inhibition of 5-CHO-THF influx in L1210, E45K, and E45K/K404E cells or inhibition of MTX influx in K404E cells (the latter measurement was made because of the higher influx of MTX than 5-CHO-THF in this cell line) (Table 2). This laboratory reported previously that the influx K_i for MTX was markedly increased, and the influx K_i for folic acid was marked decreased in E45K cells, while the influx K_i for 5-CH_3-THF was unchanged, as compared to the wild-type RFC [10,15]. Influx K_i's for MTX, 5-CH_3-THF, and folic acid in K404E cells were all increased as compared to L1210 cells; the greatest increase (21-fold) was found for 5-

Table 2
Influx inhibition constants for MTX, 5-CH_3-THF and folic acid

	MTX		5-CH_3-THF		Folic acid	
	K_i	Δ	K_i	Δ	K_i	Δ
L1210	4.4[a]	1	1.5[b]	1	240[a]	1
E45K	30[b]	6.8	1.3[b]	0.86	34[a]	0.14
K404E	39	8.7	31	21	605	2.5
E45K/K404	23	5.2	1.4	0.93	38	0.15

K_i (μM) in L1210, E45K and E45K/K404E cells was determined from Dixon plot analyses based upon inhibition of [^{3}H]-5-CHO-THF influx by MTX, 5-CH_3-THF and folic acid. K_i (μM) in K404E cells was determined from the Dixon plot analyses based upon inhibition of [^{3}H]-MTX influx by nonlabeled MTX, 5-CH_3-THF or folic acid. The data are the average of two separate experiments.
Δ: Ratio of influx K_i in transfectants to L1210 cells.
[a] From Ref. [10].
[b] From Ref. [15].

CH_3-THF. The influx K_i for MTX in E45K/K404E cells was 80% that of E45K cells, whereas influx K_i's for 5-CH_3-THF and folic acid were virtually the same as in E45K cells and far less than that in wild-type L1210 cells. Hence, for all of these folate substrates, influx kinetics approximated the E45K phenotype in the double mutants.

3.4. Effects of chloride on folate influx

One consequence of the E45K mutation was the introduction of an obligatory anion requirement for carrier function [10]. 5-CHO-THF influx in E45K cells was increased with increasing concentration of chloride, in contrast to L1210 cells in which 5-CHO-THF influx decreased as extracellular chloride concentration was increased (Fig. 4). As observed for L1210 cells, MTX influx in K404E cells decreased with increasing concentration of chloride. However, the initial drop was steeper as the chloride concentration was increased from 0 to 14 mM. 5-CHO-THF influx in E45K/K404E cells was stimulated as chloride concentration was increased, similar to what was observed for the E45K cells, but two differences were observed. (i) The percentage of maximum for 5-CHO-THF influx in chloride-free buffer for the double mutant was about twice that observed for the E45K cells (Fig. 3B). (ii) 5-CHO-THF influx in E45K/K404E cells reached its maximum at 25 mM chloride and remained constant thereafter, whereas 5-CHO-THF influx in E45K cells gradually increased as the chloride concentration increased to 110 mM.

3.5. Impact of chloride on RFC affinity for 5-CHO-THF

To further characterize the impact of alterations in extracellular chloride on transport mediated by the mutated carriers, 5-CHO-THF influx kinetic parameters in these cell lines were determined in HBS versus the chloride-free HEPES-sucrose-MgO buffer. As summarized in Table 3, in the absence of chloride the 5-CHO-THF influx K_i in L1210 cells was decreased by a factor of ~ 3, consistent with the concept that chloride is a competitive inhibitor of folate binding to RFC [24]. In the absence of extracellular chloride, the 5-CHO-THF influx K_i in K404E cells was decreased by a factor of ~ 6, an even greater reduction than in L1210 cells and consistent with the steep drop in MTX influx as chloride concentration was increased (Fig. 4). This suggests that the affinity of the K404E carrier for chloride may be greater than that of the wild-type carrier. On the other hand, the 5-CHO-THF influx K_t in E45K/E404E cells was the same in the presence and absence of chloride and was similar to what was observed for E45K cells. This indicated that the decline in influx in both lines was due to a fall in V_{max} as the chloride concentration was decreased. In the absence of chloride, the 5-CHO-THF influx V_{max} in E45K cells was decreased by a factor of 5.7, whereas the influx V_{max} in E45K/K404E cells was decreased by a factor of only 2. Hence, while the V_{max} for both carriers is

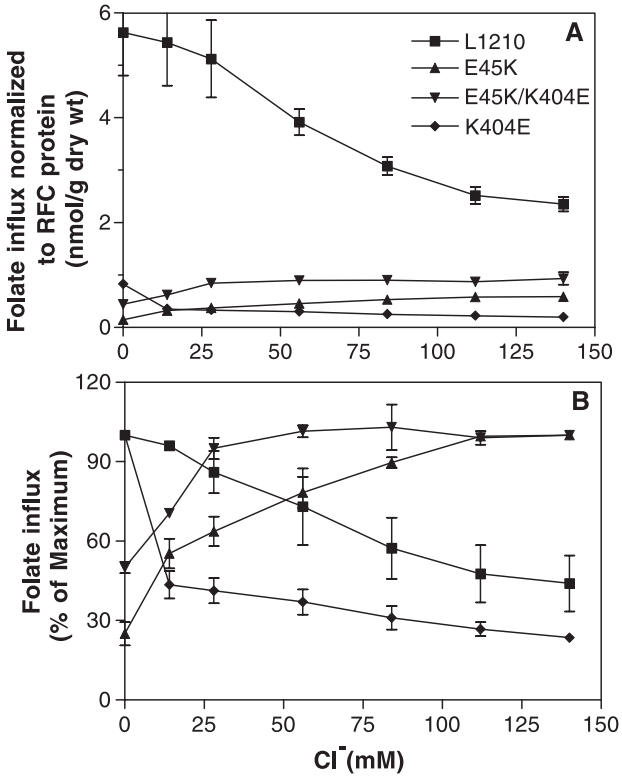

Fig. 4. Influx of [^{3}H]-5-CHO-THF or [^{3}H]-MTX as a function of chloride concentration. Cells were harvested, washed with HEPES-sucrose-MgO buffer twice and suspended with HBS, HEPES-sucrose-MgO buffer, or a mixture of HBS and HEPES-sucrose-MgO buffer. The ratio of the two buffers determined the final chloride concentration. After 25-min incubation, influx was initiated by adding 1 μM [^{3}H]-5-CHO-THF to suspensions of L1210, E45K and E45K/K404E cells or 1 μM [^{3}H]-MTX to K404E cells. Influx is the slope of initial uptake as function of time within a linear range. (A) Influx is normalized to the relative RFC expression levels indicated in Fig. 1B. (B) Influx is normalized to the maximal level of activity in each cell line. Influx in the absence of chloride for L1210 and K404E, or influx at the highest chloride concentration for E45K and E45K/K404E cells, was the maximal activity. Data are the mean ± S.E. from three separate experiments.

Table 3
Comparison of 5-CHO-THF influx kinetics in HBS and sucrose-MgO buffers

Cell lines	Influx Kinetics	HBS	Sucrose-MgO	HBS/ Sucrose-MgO
L1210	K_i	5.6	1.6	3.5
E45K	K_t	1.5 ± 0.1	1.9 ± 0.2	0.8
	V_{max}	1.42 ± 0.07	0.26 ± 0.03	5.5
K404E	K_i	55 ± 5	9.7 ± 2.2	5.7
E45K/K404E	K_t	1.5 ± 0.2	1.5 ± 0.3	1.0
	V_{max}	1.2 ± 0.1	0.61 ± 0.06	2.0

5-CHO-THF influx K_i (μM) was determined from Dixon plot analyses based upon inhibition of [^{3}]-MTX influx by 5-CHO-THF in L1210 and K404E cells. 5-CHO-THF influx K_t (μM) and V_{max} (nmol/g dry wt/min) were determined by nonlinear regression of influx versus concentration according to the Michealis–Menten equation. The K_t and V_{max} values determined in HBS (Table 1) were listed again for comparison. Data are the mean ± S.E. from three separate experiments except the K_i in L1210 cells, which is the average of two experiments with a difference of less than 15%.

influenced by chloride, the requirement for chloride by the E45K mutant appears to be greater.

4. Discussion

A previous study demonstrated that 5-CHO-THF influx was lower in cells with an E45K RFC mutation than in wild-type L1210 cells despite an increased affinity of the E45K mutant for 5-CHO-THF. This was attributed to a 12-fold decrease in the 5-CHO-THF influx V_{max} [10]. However, it was not clear whether the decreased V_{max} was the result of decreased E45K protein expression or decreased mobility of the RFC/5-CHO-5-THF complex. With the availability of polyclonal antibodies against murine RFC [21], protein expression levels in plasma membranes could now be assessed by Western blot analysis and fluorescence microscopy. The amount of E45K mutant protein in plasma membranes of E45K cells was only 30% greater than in wild-type RFC in plasma membranes of L1210 cells despite the fact that the RFC mRNA level in E45K cells was 4.5-fold greater than that in L1210 cells, suggesting that the mutation resulted in impaired translation, protein folding, and/or stability. It does not appear that the difference between mRNA and protein levels is due to impaired trafficking and insertion into the plasma membrane since E45K carrier is localized primarily to the plasma membrane. Hence, the decrease in V_{max} in E45K cells is likely due to decreased mobility of the RFC-5-CHO-THF complex. This decrease in carrier mobility could result from the introduction of a charge repulsion or attraction in the mutated carrier. The further decrease in carrier mobility in the absence of small anions, such as chloride, could be due to an alteration in the interaction between the mutated residue and another charged amino acid that increases in buffer with low ion strength and is suppressed by small anions [10,15].

Detailed characterization of murine RFC mutations identified in antifolate-resistant cells has given insight into RFC domains that are critical to binding of folates. For example, E45K [10], S46N [11], and I48F [12] substitutions selectively alter the affinity for different folates and/or the mobility of carrier-folate complexes. Hence, the first TMD, in which these three mutations are closely located, is one important determinant of folate transport. In addition to the first TMD, other TMDs have also been shown to play important roles in folate binding/translocation. For instance, a W105G mutation in the third TMD selectively increased affinity for folic acid [12], while an S309F mutation in the eighth TMD selectively decreased both affinity for MTX and the mobility of the loaded carrier [25]. An S287N mutation in the extracellular loop between the seventh and eighth TMD decreased the affinity for MTX [26]. A K404L mutation in the 11th TMD generated by site-directed mutagenesis selectively, and markedly, decreased affinity for 5-CHO-THF and 5-CH_3-THF [16]. Substitution of K411 in human RFC, corresponding to K404 in murine RFC, by leucine, glutamate, and arginine also altered substrate specificity and carrier mobility [17]. Most recently, R373 of human RFC in the 10th TMD was shown to be involved in substrate translocation but not in substrate binding [27]. The current study demonstrates that the K404E mutation in murine RFC also selectively alters influx activity for MTX and 5-CHO-THF. Hence, MTX influx mediated by the K404E mutant was slightly greater than 5-CHO-THF influx, while MTX influx mediated by wild-type RFC was half that of 5-CHO-THF influx (Fig. 3). Taken together these observations illustrate the multiple TMDs that play a role in RFC binding and translocation.

Since crystal structures have not been achieved for members of the Major Facilitator Superfamily of transporters, site-directed mutants have been utilized to infer structural relationships, best demonstrated for lactose permease from *Escherichia coli* [28]. Identification of an interaction between pairs of oppositely charged residues localized in two different TMDs indicates that these TMDs are closely packed together. For example, D237 and K358 in the lactose permease could be exchanged or simultaneously mutated to neutral residues without losing activity. If only one of the two residues was replaced with a neutral amino acid, the lactose permease was inactive [28]. Charge-

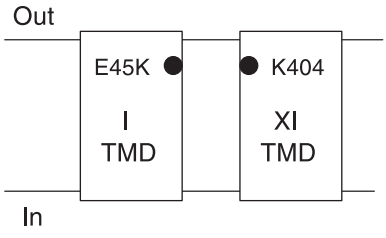

Fig. 5. Depiction of a possible interaction between E45 in the first TMD and K404 in the 11th TMD of RFC. The membrane topology of murine RFC is illustrated as predicted by Dixon et al. [31]. According this model, E45 and K404 residues, depicted by circles, are located within the first and 11th TMDs, respectively, in proximity to the extracellular interphase.

paired residues were also identified in a vesicular monoamine transporter [29]. Recently, charged-paired resides were identified in human RFC. Both the D88V in TMD 2 and K133L in TMD 4 mutants were not functional, but the D88V/R133L construct was nearly as active as wild-type human RFC [30].

In the current study, we examined a potential interaction between the E45 and K404 residues, within the first and 11th TMDs, respectively, of murine RFC using a strategy in which the charge of both residues was reversed. The data suggest an interaction between these residues in the murine carrier based upon three observations: (i) K404E had a markedly decreased affinity for all folate substrates but introduction of the second E45K mutation (in E45K/K404E cells) restored the carrier affinity for 5-CHO-THF, 5-CH_3-THF, and folic acid to the same level as that of the E45K mutant. (ii) The E45K mutant carrier had markedly reduced mobility; introduction of the second mutation doubled the mobility of carrier and the ratio of V_{max} to K_t for 5-CHO-THF was restored to 1/2 that of wild-type carrier. (iii) While chloride decreased wild-type RFC activity it increased activity of the E45K mutant. Like wild-type cells, activity of the K404E mutant increased with a decrease in chloride; while the double mutant qualitatively was similar to the E45K, the requirement for chloride was substantially decreased.

Hence, while introduction of the double mutation substantially enhanced carrier function, in particular binding to folate substrates, the overall phenotype of the E45K/K404E carrier approximated that of the E45K mutant much more than that of the K404E mutant or wild-type RFC. The impact of the K404E mutation that results in a profound loss in binding of the reduced folates, and to a lesser extent folic acid, can be reversed by the introduction of the E45K mutation in the same carrier molecule. The data therefore suggest, as illustrated in Fig. 5, that the glutamate-45 residue in the first TMD is in proximity to the lysine-404 residue in the 11th TMD close to the membrane–extracellular interface. The data indicate further that the lysine residue at position 45 in the double mutant interacts more strongly with folate substrates than the glutamate residue at position 404 and that the E45 residue is the dominant determinant of folate binding although a variety of single substitutions at the 45 position with amino acids other than lysine can sustain function of the carrier [15].

Acknowledgements

This work was supported by a Grant, CA-82621, from the National Cancer Institute.

References

[1] M.H. Saier Jr., J.T. Beatty, A. Goffeau, K.T. Harley, W.H. Heijne, S.C. Huang, D.L. Jack, P.S. Jahn, K. Lew, J. Liu, S.S. Pao, I.T. Paulsen, T.T. Tseng, P.S. Virk, J. Mol. Microbiol. Biotechnol. 1 (1999) 257–279.
[2] L.H. Matherly, I.D. Goldman, in: G. Litwack (Ed.), Membrane Transport of Folates, Elsevier Science, Academic Press, San Diego, CA, USA.
[3] R. Zhao, R.G. Russell, Y. Wang, L. Liu, F. Gao, B. Kneitz, W. Edelman, I.D. Goldman, J. Biol. Chem. 276 (2001) 10224–10228.
[4] L.H. Matherly, Prog. Nucleic Acid Res. Mol. Biol. 67 (2001) 131–162.
[5] I.D. Goldman, Ann. N. Y. Acad. Sci. 186 (1971) 400–422.
[6] G.B. Henderson, E.M. Zevely, Arch. Biochem. Biophys. 221 (1983) 438–446.
[7] P.L. Ferguson, W.F. Flintoff, J. Biol. Chem. 274 (1999) 16269–16278.
[8] S.C. Wong, L. Zhang, S.A. Proefke, L.H. Matherly, Biochim. Biophys. Acta 1375 (1998) 6–12.
[9] X. Liu, L. Matherly, Biochim. Biophys. Acta 1564 (2002) 333–342.
[10] R. Zhao, Y.G. Assaraf, I.D. Goldman, J. Biol. Chem. 273 (1998) 19065–19071.
[11] R. Zhao, Y.G. Assaraf, I.D. Goldman, J. Biol. Chem. 373 (1998) 7873–7879.
[12] A. Tse, K. Brigle, S.M. Taylor, R.G. Moran, J. Biol. Chem. 273 (1998) 25953–25960.
[13] A.J. Gifford, M. Haber, T.L. Witt, J.R. Whetstine, J.W. Taub, L.H. Matherly, M.D. Norris, Leukemia 16 (2002) 2379–2387.
[14] G. Jansen, R. Mauritz, S. Drori, H. Sprecher, I. Kathmann, M. Bunni, D.G. Priest, P. Noordhuis, J.H. Schornagel, H.M. Pinedo, G.J. Peters, Y.G. Assaraf, J. Biol. Chem. 273 (1998) 30189–30198.
[15] R. Zhao, F. Gao, P.J. Wang, I.D. Goldman, Mol. Pharmacol. 57 (2000) 317–323.
[16] I.G. Sharina, R. Zhao, Y. Wang, S. Babani, I.D. Goldman, Mol. Pharmacol. 59 (2001) 1022–1028.
[17] T.L. Witt, L.H. Matherly, Biochim. Biophys. Acta 1567 (2002) 56–62.
[18] D.W. Fry, J.C. Yalowich, I.D. Goldman, J. Biol. Chem. 257 (1982) 1890–1896.
[19] K.E. Brigle, M.J. Spinella, E.E. Sierra, I.D. Goldman, J. Biol. Chem. 270 (1995) 22974–22979.
[20] R. Zhao, I.G. Sharina, I.D. Goldman, Mol. Pharmacol. 56 (1999) 68–76.
[21] R. Zhao, F. Gao, L. Liu, I.D. Goldman, Biochim. Biophys. Acta 1466 (2000) 7–10.
[22] R. Zhao, R. Seither, K.E. Brigle, I.G. Sharina, P.J. Wang, I.D. Goldman, J. Biol. Chem. 272 (1997) 21207–21212.
[23] G.B. Henderson, E.M. Zevely, J. Biol. Chem. 259 (1984) 4558–4562.
[24] G.B. Henderson, E.M. Zevely, Biochem. Int. 6 (1983) 507–515.
[25] R. Zhao, F. Gao, I.D. Goldman, Biochem. Pharmacol. 58 (1999) 1615–1624.
[26] K. Roy, B. Tolner, J.H. Chiao, F.M. Sirotnak, J. Biol. Chem. 273 (1998) 2526–2531.
[27] H. Sadlish, F.M. Williams, W.F. Flintoff, J. Biol. Chem. 277 (2002) 42105–42112.
[28] M. Sahin-Toth, R.L. Dunten, A. Gonzalez, H.R. Kaback, Proc. Natl. Acad. Sci. U. S. A. 89 (1992) 10547–10551.
[29] A. Merickel, H.R. Kaback, R.H. Edwards, J. Biol. Chem. 272 (1997) 5403–5408.
[30] X.Y. Liu, L.H. Matherly, Biochem. J. 358 (2001) 511–516.
[31] K.H. Dixon, B.C. Lanpher, J. Chiu, K. Kelley, K.H. Cowan, J. Biol. Chem. 269 (1994) 17–20.